Monitoring Soil Moisture Deficit Effects on Vegetation Parameters Using Radiative Transfer Models Inversion and Hyperspectral Measurements Under Controlled Conditions

Bagher Bayat [(1)], Christiaan Van der Tol[(1)], Wouter Verhoef [(1)]

[(1)] Faculty of Geo-Information Science and Earth Observation (ITC), University of Twente, P.O. Box 217, 7500 AE Enschede, The Netherlands. Email:b.bayat@utwente.nl

ABSTRACT

Plant-available soil moisture is a key element which affects plant properties in their ecosystems. This study shows *Poa pratensis* -a species of grass- responses to soil moisture deficit during an artificial drought episode in a greenhouse experiment. We used radiative transfer model inversion to monitor the gradual manifestation of soil moisture deficit effects on vegetation in a laboratory setting. Plots of 21 cm x 14.5 cm surface area with *Poa pratensis* plants that formed a closed canopy were subjected to water stress for 40 days. In a regular weekly schedule, canopy reflectance was measured. The 1-D bidirectional canopy reflectance model SAIL, coupled with the leaf optical properties model PROSPECT, was inverted using hyperspectral measurements by means of an iterative optimization method to retrieve vegetation biophysical and biochemical parameters (mainly; LAI, Cab, Cw, Cdm and Cs). The relationships between these retrieved parameters with soil moisture content were established in two separated groups; stress and non-stressed. All parameters retrieved by model inversion using canopy spectral data showed good correlation with soil moisture content in the drought episode. These parameters co-varied with soil moisture content under the stress condition (Chl: R^2= 0.91, Cw: R^2= 0.97, Cs: R^2= 0.88 and LAI: R^2=0.48) at the canopy level.

Keywords: Soil moisture deficit; water stress; vegetation responses; canopy spectra; model inversion; quantitative remote sensing

1. INTRODUCATION

One of the applications of quantitative remote sensing is to quantify the physiological responses of plants to various environmental conditions [1]. The use of optical remote sensing data requires an understanding of vegetation spectral reflectance as governed by leaf composition, structure, and canopy architecture. There is valuable information in the reflectance spectra that relates to the biophysical and biochemical properties of both the leaf and the canopy [2]. Monitoring spectral changes over time, translating spectra into biophysical and biochemical parameters of interest, and relating these parameters to environmental stresses are three main aspects of vegetation remote sensing [3].

Among environmental stresses, soil moisture deficit or "ecological drought" is particularly relevant to plant communities [4,5]. Vegetation in natural ecosystems will face severe water stress as a response to repeated drought episodes. A harsh drought condition for a plant is defined in terms of soil water content and not necessarily by rainfall scarcity, so that soil characteristics can play a role in the ecosystem and the plant can experience drought even under favourable weather conditions [6]. In many ecosystems - especially in arid and semi-arid climates - soil moisture deficit is often the most important stress factor for vegetation communities.

Progress of drought can be efficiently tracked by monitoring three major successive phases during a water stress episode [7]. During phase I, plant biophysical processes, such as evapotranspiration and photosynthesis, proceed as in well-watered conditions until soil moisture declines and cannot meet evapotranspiration demand. This might usually happen when soil water content decreases by 50% [8]. Hereafter, drought enters phase II. In this step, biophysical processes of the plant are reduced to lower than the potential levels. Vegetation transpiration, photosynthesis and water relations, which are sensitive to water potential at this stage, depend on soil properties, atmospheric condition and the plant factors. By decreasing soil water content, drought will progress and enter phase III. Although at this phase all stomata are totally closed, still some water is lost by non-stomatal processes; from (1) the cuticle surface into the atmosphere and (2) roots into extremely dry soil [8,9]. At this phase, vegetation has already reached its permanent wilting point and cannot longer survive and recover. As a result, all aspects of vegetation growth (including physiological and biochemical processes) are affected [10]. Thus, in water stress condition through a drought episode, changes take place in biochemical, biophysical, physiological aspects of plants.

During these phases, optical signals reflected by the plant will change and the reflectance spectra of the leaves will respond to the stress [11]. The fact that these changes occur over the entire reflectance spectrum, especially in the pigment absorption bands, in the near infrared (NIR) and at the water absorption bands, makes spectroscopy a valuable tool in assessing stress-induced impacts on plants [2].

To translate spectral remote sensing data into vegetation biophysical and chemical parameters, specialized algorithms and approaches are needed. There are two common approaches: the statistical approach [12–14] and physical modeling [15–18]. Statistical approaches include spectral vegetation indices computation and regression models applications, which are based on using data from various spectral bands. In many studies, plant stress effects have been analyzed by regressions against vegetation indices [11,19]. The physical approach consists of applying radiative transfer models (RTM) that are based on physical laws. They are highly suited for studying the relationship between biophysical variables and reflectance spectral data [20,21] since they are not site, sensor and species-specific and offer an explicit relationship between spectral signature and vegetation properties.

Physical approaches have been widely used to retrieve vegetation parameters from various types of remote sensing data [15–18,22]. Physical modelling of vegetation remote sensing signals reveals the links that exist between vegetation biophysical and biochemical variables on the one hand and the leaf and canopy spectral reflectance on the other.

In this study, physical approaches have been employed to retrieve the biophysical and biochemical parameters of vegetation (LAI, Cab, Cw, Cs) from hyperspectral measurements by inversion of the widely used PROSPECT and SAIL models to analyze the effects of prolonged soil water deficit on grass. Following this, the relationship between retrieved parameters and soil moisture content was assessed and compared to a control group with no soil water deficit. In this way, we could monitor drought-induced impacts on vegetation using a radiative transfer model inversion. To reach these objectives, we conducted a laboratory experiment in which 30 pots with *Poa pratensis* grass equipped with recording soil moisture sensors were monitored with frequent hyperspectral measurements at the canopy level.

2. MATERIALS AND METHOD

2.1. Experimental setup

During this research, a greenhouse experiment was conducted for about 40 days in the garden of the ITC faculty of the University of Twente. A grass carpet (of *Poa pratensis*) grown locally was cut into 60 rectangles and transplanted into 21x14.5 cm pots with a depth of 12 cm, all filled with organic soil. All 60 pots were watered regularly until the canopy height was about 15 cm after which they were placed in a greenhouse. The greenhouse shielded the vegetation from rainfall, but temperature, irradiance and humidity were not controlled. We selected grass for our experiments because of its rapid response to soil moisture deficits, and because the requirements applying a 1-D vertical model like SAIL are more easily met for relatively small canopies. The pots were divided into three equally sized groups: (1) a group under the well-watered condition; (2) a group under a reduced watering condition; and (3) a group that was not irrigated at all. Ten pots in each group were equipped with calibrated soil moisture sensors (Em50 Series, Decagon Devices, Inc, USA). The well-watered pots were irrigated weekly with 200-250 ml water, such that the volumetric soil moisture content fluctuated around 30-40%. The pots in the reduced water treatment were watered weekly with about 100-200 ml water, such that the volumetric soil moisture content declined over the duration of the experiment to a value of 15-30%. The pots subject to no water treatment were not irrigated in order to expose them to maximum water stress conditions. The greenhouse was fitted with removable plastic covers as walls, which were left open during daytime and closed during the night and rainfall events.

2.2. Instrumentation and measurements

2.2.1. Canopy hyperspectral reflectance measurements

Canopy spectra of all pots was measured in a remote sensing laboratory in a dark room using the Analytical Spectral Devices, FieldSpec® 3 Hi-Res Portable Spectroradiometer in Full Range (ASD Inc., Boulder CO., USA) that acquires continuous spectra located in the VIS, NIR and SWIR regions (350 to 2500 nm). The plants were illuminated by four tungsten halogen quartz lamps of 100W, each installed to be pointing in four azimuth directions, each under a 45 degree zenith incidence angle. Measurements were taken at the sampling intervals of the instrument (1.4 nm - VIS and NIR; 2nm - SWIR) and were resampled by the instrument automatically into 1 nm intervals using linear and polynomial interpolations [23]. The sensor had a fiber optic cable with a 25 degree field of view. The fiber optic cable was placed in a pistol and mounted on a stand. In the setting, under 22.55 cm height and 25 degrees FOV, the spectrometer scanned a diameter of 10 cm on the pot surface with the nadir point at the center of the circle.

2.2.2. Soil hyperspectral reflectance measurements

Reflectance of the background soil containing various ranges of soil moisture content was also measured. These spectroradiometer measurements were used as inputs in the radiative transfer modelling. At the end of the experiment, all biomass of 10 samples was completely harvested in order to take soil reflectance measurements on a set of soil samples having a range of soil moisture.

2.2.3. Leaf Area Index and leaf chlorophyll content

LAI was measured directly during the experiment at

different dates (having various soil moisture contents) by harvesting the pot samples which did not have a soil moisture sensor. Leaf area was measured on a representative sub-sample in the pot and related to its dry mass (oven dried at 65°C for 48 hours). The ratio of leaf area to leaf dry mass, known as specific leaf area, was calculated in $cm^2\ g^{-1}$. Finally, the total dry mass of leaves collected within the pot surface area was converted into LAI by multiplying by the specific leaf area. To take measurements of leaf chlorophyll content, we used the Minolta SPAD-502 leaf chlorophyll meter. We took 10 chlorophyll samples from each pot during one measurement located in the field of view of the canopy reflectance measurements and used the average value. The relative values of the SPAD 502 were converted into absolute amount of chlorophyll using a widely-used calibration curve from the literature [24].

2.2.4. Soil water characteristic (SWC) curve

Soil water characteristic curve was used to define the water stress threshold for plants in the experiment. This curve relates the mass or volume of water retained in a soil under equilibrium conditions to matric potential [25]. It depends on the soil type, structure, distribution of pore spaces and organic content. The SWC curve was obtained by measuring the water potential and volumetric soil moisture on a set of soil samples that had a range of water contents. We used the WP4C Dew Point Potentiameter (Decagon Devices, Inc, WP4C, USA) to quantify the water potential of the samples. The volumetric soil moisture of the same samples was measured along with the water potentials. By plotting pF (log of the negative water potential in cm) against soil moisture ($m^3\ m^{-3}$), the SWC curve of the samples was generated [26]. We used soil moisture content corresponding to a pF of 4.2 as a stress threshold, since the permanent wilting point of the used soil type in this experiment, organic soil, is near this pF value [27–29].

2.3. Inversion of Radiative Transfer Models

Implementations of the well-known and widely used PROSPECT and SAIL radiative transfer models were selected for physically based leaf and canopy parameters retrieval. We used the so-called RTMo model, which is a four-stream SAIL model for the radiative transfer of incident light in canopies [30]. RTMo is a combination of the '4SAIL' model [31] with a few additions, and the leaf radiative transfer model 'Fluspect' which is basically the 'PROSPECT5' model with a few modifications and additions. The main differences between RTMo (4SAIL+ Fluspect) and PROSAIL (SAILH+PROSPECT4) are: (1) The leaf angle distribution in RTMo is described with two parameters, the mean leaf inclination parameter (LIDFa) and the bimodality of the leaf inclination distribution (LIDFb), while PROSAIL uses only the Mean Leaf Inclination Angle (MLA); (2) the fraction of diffuse incoming solar radiation is spectral-dependent while in PROSAIL it is considered as a constant value.

Retrieval of canopy parameters from hyperspectral canopy level measurements was performed by inverting the RTMo model. The PROSPECT5 model [32,33] calculates the leaf hemispherical reflectance and transmittance as a function of four input parameters: (1) the leaf structural parameter N (unitless); (2) the leaf chlorophyll a+b concentration Cab ($\mu g\ cm^{-2}$); (3) the dry matter content Cdm ($g\ cm^{-2}$); and (4) the water concentration of the leaves Cw ($g\ cm^{-2}$). In Fluspect also brown pigment concentration, Cs (arbitrary unit), is included. The 4SAIL model [15,16] is a one-dimensional bidirectional turbid medium radiative transfer model. It defines the canopy as a horizontally homogenous layer that consists of small vegetation elements. The model has been applied successfully to homogeneous vegetated canopies [15,34]. In addition to the leaf reflectance and transmittance, the RTMo model requires some other input parameters to simulate the top-of-canopy bidirectional reflectance. These are the sun zenith angle, θ_s (deg); the sensor viewing angle, θ_o (deg); the relative azimuth angle between sensor and sun, ψ (deg); solar irradiance, E_{sun}; sky irradiance, E_{sky}, background reflectance (soil reflectance) for each wavelength, r_{sl}; LAI ($m^2\ m^{-2}$); the hot spot size parameter, defined as the ratio between the average width of the leaves and the canopy height [35] and the leaf inclination distribution function (LIDF) which is described with 2 parameters: the mean leaf inclination parameter (LIDFa) and bimodality of the leaf inclination distribution (LIDFb).

Inversion of a physical reflectance model results in finding the set of input parameters which leads to the best match between simulated spectra by the model and observed spectra by the sensor. In this research we used an iterative optimization technique for model inversion. The iterative optimization is a classical technique to invert any model with continuous variables. It has been applied as well to invert radiative transfer models in remote sensing [36]. The minimization of a merit function that accounts for the differences between the simulated and the measured reflectance spectra is used as a stopping criterion for this optimization problem.

Table 1 shows the initial guess of input parameters used in this research. To consider the contribution of the background soil reflectance in the model inversion, we changed the model soil spectra based on the value of soil moisture recorded in the pot in which canopy reflectance were taken.

Table 1. Initial guess of parameters for retrieval

Parameter	Abbr. in model	Unit	Initial guess
Leaf chlorophyll content	Cab	$\mu g\ cm^{-2}$	40
Leaf water content	Cw	$g\ cm^{-2}$	0.009
Leaf dry matter content	Cdm	$g\ cm^{-2}$	0.012
Leaf area index	LAI	$m^2\ m^{-2}$	1
Senescent material	Cs	-	0
Leaf structural parameter	N	-	1.5
Leaf inclination parameter	LIDFa	-	- 0.35
Biomodality of the leaf inclination	LIDFb	-	- 0.15
carotenoids	Cca	$\mu g\ cm^{-2}$	5
Hot spot size parameter	hot	$m\ m^{-1}$	0.05
solar zenith angle	θ_s	deg	45
observation zenith angle	θ_o	deg	0
Relative Azimuth Angle	ψ	deg	0

The cost function calculated was simply the sum of the squared differences over the whole wavelength range of the measured reflectance. From the result, the RMSE between measured and simulated spectra was calculated according to Eq. 1:

$$RMSE = \sqrt{\frac{\sum_{i=1}^{n}(R_{measured} - R_{simulated})^2}{n}} \quad (1)$$

where $R_{measured}$ is a measured reflectance and $R_{simulated}$ is a simulated reflectance through inversion, and n is the number of wavelengths.

3. RESULTS AND DISCUSSION

3.1. SWC curve as the water stress threshold

The SWC curve measured in the laboratory (Fig. 1) was used to define a threshold for water stress. Common values of the pF (log of the negative water potential in cm) for the onset of stress and for the permanent wilting point are 2.6 and 4.2, respectively. Fig. 1 shows that these occur at volumetric soil moisture contents of 0.23 and 0.2 [$m^3\ m^{-3}$]. Because the *Poa pratensis* did not show any signs of drought stress for values of pF below 4.2, we used a soil moisture condition of 0.2 [$m^3\ m^{-3}$] as an upper limit for stress.

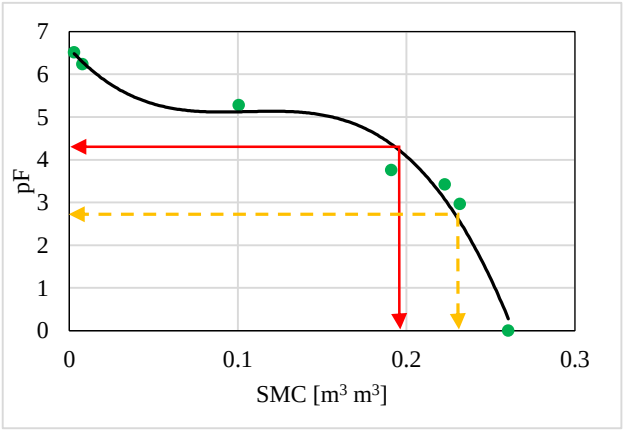

Figure 1. Soil Water Characteristics (SWC) curve produced in the laboratory and stress thresholds

3.2. RTMo Radiative Transfer Modelling

3.2.1. RTMo Inversion Results

The RMSE of measured and simulated spectra was employed as the criterion of the model inversion performance. Fig. 2 shows the goodness of fit of the simulation in some samples of measured and simulated canopy reflectance spectra on different days of the experiment.

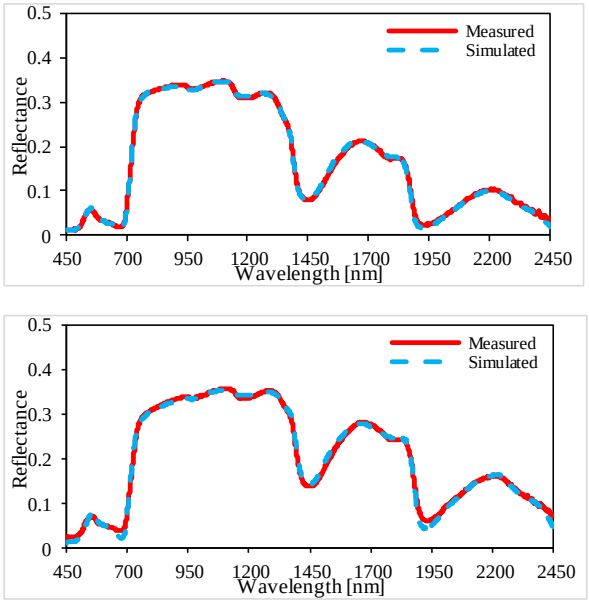

Figure 2. Measured (red line) and simulated/modeled (blue dash line) canopy spectra in different phases of drought experiment.

These examples represent the performance of the inversion since there was a full agreement with the measured and simulated reflectance. The small error in the model inversion ($0.002 < RMSE < 0.009$) confirmed the simulation performance under different soil moisture

contents during the experiment. However, the inversion results were also evaluated in their accuracy (deviations from measured parameter values). The relation between the measured and the retrieved (estimated) parameters (Cab and LAI) is demonstrated in Fig. 3. This figure illustrats the deviatins from the one-to-one line. There was a significant relationship between measured and retrieved values.

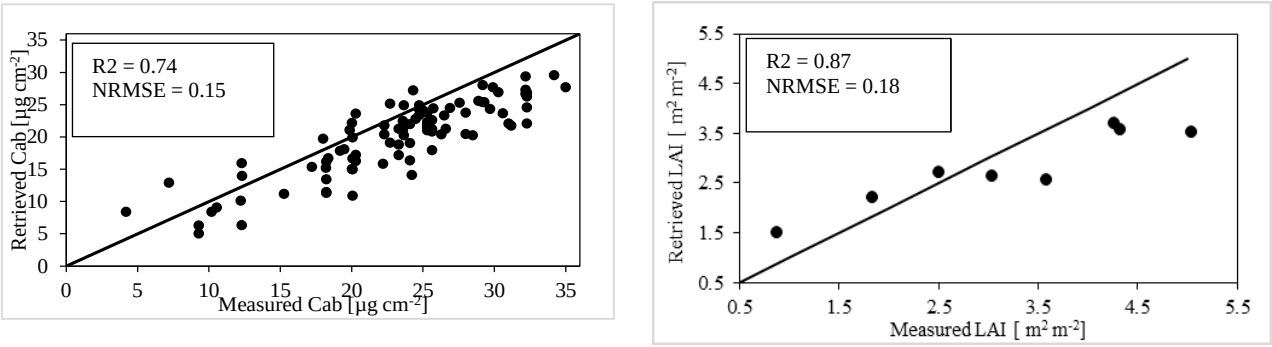

Figure 3. Retrieved versus measured vegetation parameters; (left) leaf chlorophyll content, and (right) LAI.

3.2.2. Trend of Retrieved Parameters

Retrieved leaf and canopy (leaf multiplied by LAI) parameters were plotted against their related soil moisture (Fig. 4). This way, we could follow the trend of changes and detect water stress impacts on the retrieved parameters. In the left panels of Fig. 4, we pooled together all the samples and fitted a nonlinear curve while in the middle and right panels in Fig. 4 we separated stressed and control treatments and fitted separate straight line segments. As Fig. 4 clearly shows (based on statistical analysis results shown in Table 2) the relationships are strong and significant, in the stressed treatment (SMC < 0.2). The chlorophyll content of the leaf is declining. Healthy plants, of which the growth is not limited by water availability, are generally expected to have higher chlorophyll content than water stressed plants. Reduced chlorophyll concentration is often associated with the stressed plants. In addition, the water content of the leaf, leaf dry matter content and LAI showed a declining trend during the water stress episode while Cs (brown pigments) showed an increasing trend. The trend of parameter changes at the canopy level indicates that at the permanent wilting point, all pigments and physical properties start changing and brown leaves appear. Furthermore, the results of the retrievals have shown no significant changes in control treatments either at leaf or canopy level. Simple linear regression was performed between different retrieved parameters (at leaf and canopy levels) and soil moisture content in stressed and non-stressed treatments (Tab. 2). ANOVA analysis showed that all relationships in the stressed treatments (n = 51) were strong (acceptable R^2 values) and significant (the F-ratio for the slopes were significant at the 0.05 critical alpha level) at both leaf and canopy scale while there were not any significant relationships in the control (n = 56) treatment (low R^2 values and no significant F-ratio for the slopes). In addition, two-samples t-test results showed that there were significant differences between the stressed and control treatments at both leaf and canopy scale. When we pooled together all the samples, nonlinear regression was performed for all measurements together.

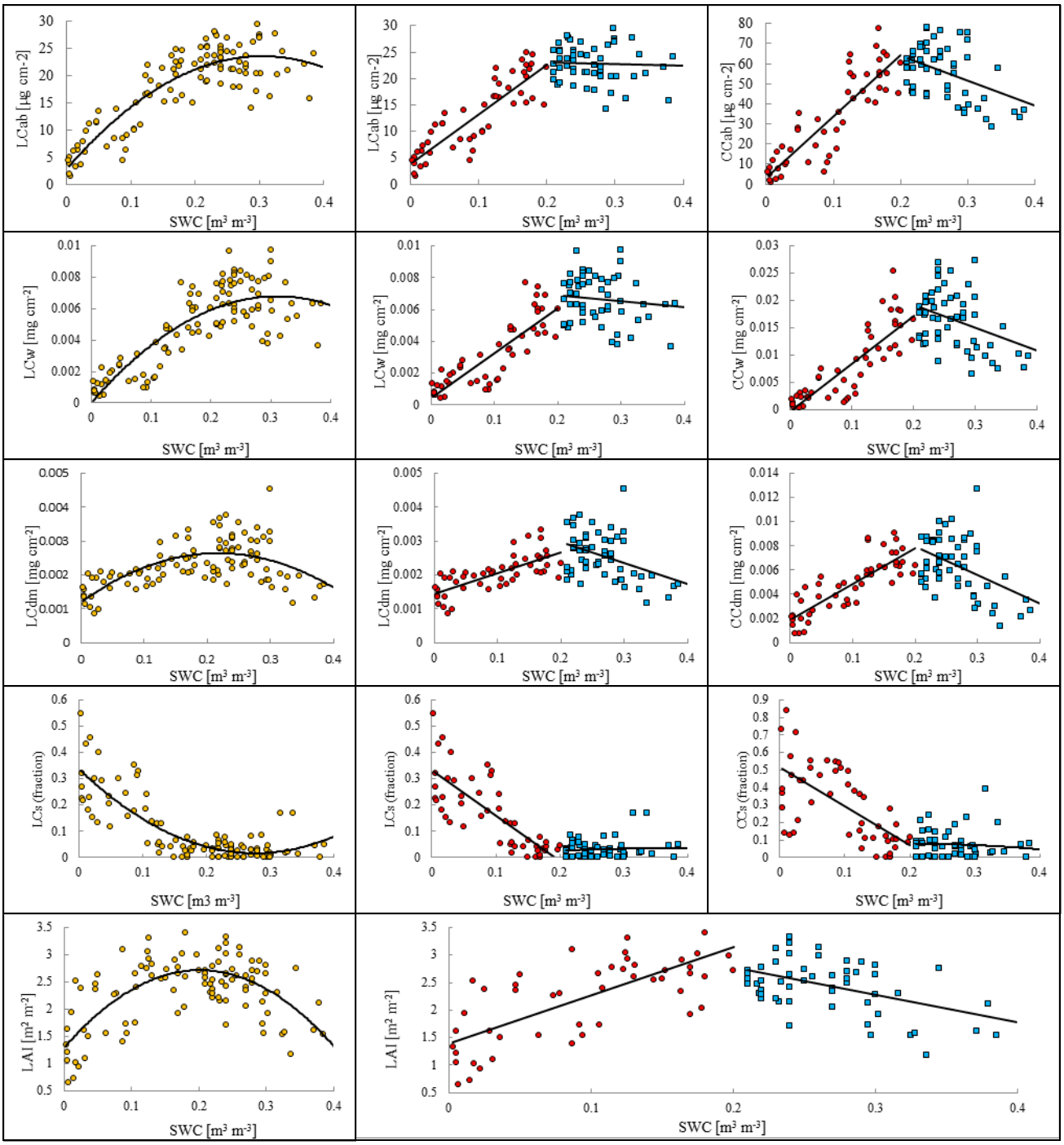

Figure 4. Relationship between retrieved parameters and soil moisture content; Left panels show all parameter changes together at leaf level, the middle panels show the parameter changes at the leaf level seperated by water stress threshold (SWC = 0.2 [m3 m^{-3}], pF > 4.2) and the right panels show canopy (leaf level multiplied by LAI) parameter changes.

Table 2. Relationship established between retrieved parameters (canopy levels) and soil moisture content in the stressed and control treatments.

relationships/analysis		One-way ANOVA				Two samples t-test (differences of treatments)
relationship	Treatment	R^2	RMSE	F-ratio	probability	p-value (Two-tailed)
Retrieved canopy parameters:						
Cab-SWC	Stressed	0.76	10.89	154.677	**<0.0001***	**0.0001***
	control	0.19	12.09	13.268	0.001	
Cw-SWC	Stressed	0.72	0.004	122.35	**<0.0001***	**0.0001***
	control	0.15	0.005	9.36	0.003	
Cdm-SWC	Stressed	0.69	0.001	106.496	**<0.0001***	**0.001***
	control	0.23	0.002	16.125	0.0001	
Cs-SWC	Stressed	0.42	0.167	35.141	**<0.0001***	**0.0001***
	control	0.008	0.006	0.456	0.501	
LAI-SWC	Stressed	0.52	0.53	52.384	**<0.0001***	0.14*
	control	0.22	0.444	15.82	0.001	
	together	0.44	0.48	-	-	-

*The probability less than 0.05 (and acceptable correlation based on R-suared) is deemed significant (and strong) and denoted by bold number and star

As Fig. 4 and Table 2 show, the trend of the parameter changes is totally different in stressed treatments in comparison to the control treatment. There is a strong and significant relationship between parameters and soil moisture content in the stress treatment. Cab, Cw, Cdm and LAI are declining during soil moisture deficit but Cs is increasing. However, such relationships in the control treatment are neither strong nor significant. LAI has a significant correlation with soil moisture content, but it is not strong. This LAI trend might be explained by taking the time into account. We performed this experiment in late August and September when the growth period of vegetation is influenced by the season. September is the time when LAI of well-watered plants is also decreasing. The retrieved parameters showed a significant relationship with soil moisture content for the stress treatment. Almost all the retrieved parameters values (except Cs) are declining while the soil is drying. The more away from the stress threshold (and therefore, the dryer the soil and consequently the more severe the drought), the lower the parameters values. Thus, the soil moisture at the permanent wilting point might be a valuable index in which we can find a significant relationship between the parameters and the soil moisture content. In addition, corresponding retrieved parameter values at the wilting point (in this study a soil moisture content of 0.2 [m^3 m^{-3}]) might be a useful indicator of severity of drought and could be used as drought signals when measurements of soil moisture in the field are not available.

4. CONCLUSIONS

In this study, we investigated in the laboratory the vegetation response to water stress in a *Poa pratensis* grass canopy exposed to various levels of soil moisture deficit. Spectroradiometer observations and modeling simulations described in this article demonstrate that water stress changes all parts of the reflectance spectrum (VIS, NIR and SWIR). A 40% decrease in soil moisture content in a drought episode results in an average increase of 65% (std = 0.02) in reflectance in the visible part (450 - 700 nm), of 9% (std = 0.05) in the NIR part (700 - 1300 nm) and of 60% (std = 0.07) in the SWIR part (1300 - 2450 nm). Furthermore, we retrieved leaf and canopy parameters using RTMo with satisfactory accuracy. By investigation of the trends of parameter changes during the experiment (both lab measurements and modelling results), we concluded that the soil moisture content at the permanent wilting point marked the threshold in which different behaviour of stressed and control treatments could be identified. Although there are some effects of soil moisture deficit on vegetation properties at soil moisture contents greater than the permanent wilting point, we found that the relationship between soil moisture deficit and vegetation properties changes were strong and significant below our proposed threshold (pF value below 4.2 and soil moisture lower than 0.2 [m^3 m^{-3}]). Corresponding retrieved parameter values in the proposed threshold might be a useful detector of drought signals when the measurements of soil moisture in the field is not available. Although a pF of 2.60 to 4.2 is the point from which water uptake starts decreasing, this research showed that it is not detectable in the VIS, NIR and SWIR parts of the spectrum.

REFERENCES

1. Muttiah, R. S. *From laboratory spectroscopy to remotely sensed spectra of terrestrial ecosystems*; Springer Science & Business Media, 2002.
2. Barton, C. V. M. Advances in remote sensing of plant stress. *Plant Soil* **2011**, *354*, 41–44.
3. Meroni, M.; Colombo, R.; Panigada, C. Inversion of a radiative transfer model with hyperspectral observations for LAI mapping in poplar plantations. *Remote Sens. Environ.* **2004**, *92*, 195–206.
4. Zhou, S.; Duursma, R. a.; Medlyn, B. E.; Kelly, J. W. G.; Prentice, I. C. How should we model plant responses to drought? An analysis of stomatal and non-stomatal responses to water stress. *Agric. For. Meteorol.* **2013**, *182-183*, 204–214.
5. Wolf, S.; Eugster, W.; Ammann, C.; Häni, M.; Zielis, S.; Hiller, R.; Stieger, J.; Imer, D.; Merbold, L.; Buchmann, N. Contrasting response of grassland versus forest carbon and water fluxes to spring drought in Switzerland. *Environ. Res. Lett.* **2013**, *8*, 035007.
6. Porporato, A.; Laio, F.; Ridol, L.; Rodriguez-iturbe, I. Plants in water-controlled ecosystems : active role in hydrologic processes and response to water stress III . Vegetation water stress. **2001**, *24*, 725–744.
7. Sinclair, T. R.; Ludlow, M. M. Influence of soil water supply on the plant water balance of four tropical grain legumes. *Funct. Plant Biol.* **1986**, *13*, 329–341.
8. Blum, A. Crop responses to drought and the interpretation of adaptation. *Plant Growth Regul.* **1996**, *20*, 135–148.
9. Grantz, D. A. Plant response to atmospheric humidity. *Plant. Cell Environ.* **1990**, *13*, 667–679.
10. Da Silva, E. C.; de Albuquerque, M. B.; Azevedo Neto, A. D. de; Silva Junior, C. D. da Drought and Its Consequences to Plants – From Individual to Ecosystem. **2013**.
11. de Jong, S. M.; Addink, E. a.; Hoogenboom, P.; Nijland, W. The spectral response of Buxus sempervirens to different types of environmental stress – A laboratory experiment. *ISPRS J. Photogramm. Remote Sens.* **2012**, *74*, 56–65.
12. Colombo, R.; Bellingeri, D.; Fasolini, D.; Marino, C. M. Retrieval of leaf area index in different vegetation types using high resolution satellite data. *Remote Sens. Environ.* **2003**, *86*, 120–131.
13. Baret, F.; Guyot, G. Potentials and limits of vegetation indices for LAI and APAR assessment. *Remote Sens. Environ.* **1991**, *35*, 161–173.
14. Darvishzadeh, R.; Atzberger, C.; Skidmore, A.; Schlerf, M. Mapping grassland leaf area index with airborne hyperspectral imagery: A comparison study of statistical approaches and inversion of radiative transfer models. *ISPRS J. Photogramm. Remote Sens.* **2011**, *66*, 894–906.
15. Verhoef, W. Light scattering by leaf layers with application to canopy reflectance modeling: the SAIL model. *Remote Sens. Environ.* **1984**, *16*, 125–141.
16. Verhoef, W. Earth observation modeling based on layer scattering matrices. *Remote Sens. Environ.* **1985**, *17*, 165–178.
17. Verhoef, W.; Bach, H. Remote sensing data assimilation using coupled radiative transfer models. *Phys. Chem. Earth, Parts A/B/C* **2003**, *28*, 3–13.
18. Verhoef, W.; Bach, H. Coupled soil–leaf-canopy and atmosphere radiative transfer modeling to simulate hyperspectral multi-angular surface reflectance and TOA radiance data. *Remote Sens. Environ.* **2007**, *109*, 166–182.
19. Zhang, Y.; Peng, C. H.; Li, W. Z.; Fang, X. Q.; Zhang, T. L.; Zhu, Q. A.; Chen, H.; Zhao, P. X. Monitoring and estimating drought-induced impacts on forest structure, growth, function, and ecosystem services using remote-sensing data: recent progress and future challenges. *Environ. Rev.* **2013**, *21*, 103–115.
20. Clevers, J. G. P. W.; Kooistra, L.; Schaepman, M. E. Estimating canopy water content using hyperspectral remote sensing data. *Int. J. Appl. Earth Obs. Geoinf.* **2010**, *12*, 119–125.
21. Atzberger, C.; Richter, K.; Vuolo, F.; Darvishzadeh, R.; Schlerf, M. Why confining to vegetation indices? Exploiting the potential of improved spectral observations using radiative transfer models. *Proc. SPIE* **2011**, *8174*, 81740Q.
22. Jacquemoud, S.; Bacour, C.; Poilve, H.; Frangi, J.-P. Comparison of four radiative transfer models to simulate plant canopies reflectance: Direct and inverse mode. *Remote Sens. Environ.* **2000**, *74*, 471–481.
23. Borzuchowski, J.; Schulz, K. Retrieval of Leaf Area Index (LAI) and Soil Water Content (WC) Using Hyperspectral Remote Sensing under Controlled Glass House Conditions for Spring Barley and Sugar Beet. *Remote Sens.* **2010**, *2*, 1702–1721.
24. Markwell, J.; Osterman, J.; Mitchell, J. Calibration of the Minolta SPAD-502 leaf chlorophyll meter. *Photosynth. Res.* **1995**, 467–472.
25. Tuller, M.; Or, D. Retention of water in soil and the soil water characteristic curve. *Encycl. soils Environ.* **2004**, *4*, 278–289.
26. Decagon Devices, I. M. *Dewpoint PotentiaMeter Operator's Manual*; 2010.
27. da Costa, B. The pF at the Wilting Point of Several Indiana Soils1. **1946**.
28. Parent, L. E.; Ilnicki, P. *Organic soils and peat materials for sustainable agriculture*; CRC Press, 2002.
29. Fredlund, D. G.; Xing, A. : Equations for the soil-water characteristic curve. *Can. Geotech. J.* **1994**, *31*, 1026–1026.
30. Van der Tol, C.; Verhoef, W.; Timmermans, J.; Verhoef, A.; Su, Z. An integrated model of soil-canopy spectral radiances, photosynthesis, fluorescence, temperature and energy balance. *Biogeosciences* **2009**, *6*, 3109–3129.
31. Verhoef, W.; Jia, L.; Xiao, Q.; Su, Z. Unified Optical-Thermal Four-Stream Radiative Transfer Theory for Homogeneous Vegetation Canopies. *IEEE Trans. Geosci. Remote Sens.* **2007**, *45*, 1808–1822.
32. Jacquemoud, S.; Baret, F. PROSPECT: A model of leaf optical properties spectra. *Remote Sens. Environ.* **1990**, *34*, 75–91.
33. Jacquemoud, S.; Ustin, S. L.; Verdebout, J.; Schmuck, G.; Andreoli, G.; Hosgood, B. Estimating leaf biochemistry using the PROSPECT leaf optical properties model. *Remote Sens. Environ.* **1996**, *56*, 194–202.
34. Jacquemoud, S.; Verhoef, W.; Baret, F.; Bacour, C.; Zarco-Tejada, P. J.; Asner, G. P.; François, C.; Ustin, S. L. PROSPECT+SAIL models: A review of use for vegetation characterization. *Remote Sens. Environ.* **2009**, *113*, S56–S66.
35. Verhoef, W.; Bach, H. Coupled soil–leaf-canopy and atmosphere radiative transfer modeling to simulate hyperspectral multi-angular surface reflectance and TOA radiance data. *Remote Sens. Environ.* **2007**, *109*, 166–182.
36. Pragnere, a.; Baret, F.; Weiss, M.; Myneni, R.; Knyazikhin, Y.; Wang, L. B. Comparison of three radiative transfer model inversion techniquesto estimate canopy biophysical variables from remote sensing data. *IEEE 1999 Int. Geosci. Remote Sens. Symp. IGARSS'99 (Cat. No.99CH36293)* **1999**, *2*, 9–11.